CRYSTAL GROWTH & DESIGN
2009
VOL. 9, NO. 2
1164–1169

Controlled Growth of Parallel Oriented ZnO Nanostructural Arrays on Ga_2O_3 Nanowires

Lena Mazeina,* Yoosuf N. Picard, and Sharka M. Prokes

Electronics Science and Technology Division, Naval Research Laboratory, 4555 Overlook Avenue, Washington, D.C. 20375

Received September 5, 2008; Revised Manuscript Received November 6, 2008

ABSTRACT: Novel hierarchical ZnO−Ga_2O_3 nanostructures were fabricated via a two stage growth process. Nanowires of Ga_2O_3 were obtained in the first stage by the vapor−liquid−solid mechanism and used as the foundation for growth of self-assembled, ordered arrays of ZnO nanostructures during the second stage by the vapor−solid mechanism. The resulting hierarchical nanostructures had a final morphology consisting of nanobrushes (NBs) with Ga_2O_3 as the core and ZnO as the branches self-assembling symmetrically in six equiangular directions around the core. Characterization of the NBs was performed by scanning and transmission electron microscopies, energy dispersive spectroscopy, and Fourier transform infrared spectroscopy. The mechanism of formation is discussed together with potential applications, among which is the aligned growth of vertically aligned ZnO nanorods that are touted for optoelectronics. Advantages of this alignment method are lower temperature growth, reduced amount of thermally induced defects, and absence of catalytic impurities.

Introduction

With an ever growing list of potential applications, there is a greater demand for developing new methods for producing nanostructures (NS) with diverse and tunable properties. Often materials properties can be modified by the addition of other materials with complementary properties to form core−shell, hetero- and/or doped structures. These methods can tune materials to the desired properties, as well as help to achieve multifunctionality. Therefore, much work has recently focused on developing approaches for synthesizing NS consisting of different materials, including ZnO and Ga_2O_3. These semiconducting oxides find many potential applications in optoelectronics, near UV-lasers, photonics, and gas sensors.[1,2] Many of these applications depend on, and can be reinforced by, the controlled and reproducible alignment of NS with well-defined morphologies.[2] For example, needle-like ZnO NS show excellent field emission characteristics[3,4] because of the extreme sharpness of the tips. However, creating ordered or aligned patterns in high-density arrays is still a challenge.[5] Although a variety of methods for obtaining laterally aligned NS exist,[5−7] techniques for the synthesis of vertically aligned NS are limited. Currently, the most successful method for fabricating vertically aligned parallel NS is a growth based on an epitaxial relationship between the substrate and the NS.[1−3] Many of these methods require high temperatures (>800 °C),[2] at which additional thermally induced defects form in oxides with variable composition (e.g., ZnO),[8,9] and a catalyst (e.g., VLS growth) which might introduce undesired impurities or dopants.[1,3] However, methods that do not require high temperatures and catalyst assistance need additional processing so that every single nanorod has a contact to a conductive pathway.

Another promising method for creating ordered and/or aligned patterns of NS is the controlled growth of hierarchical NS. Although there is a large variety of hierarchically branched morphologies, only those where branches self-assemble regularly and symmetrically around the core are most promising for controlled growth of aligned NS. Such heterostructures have been obtained by growth of ZnO,[10−13] Ga_2O_3,[14] SnO_2,[15] and GaAs[16] nanorod branches symmetrically around the nanowire (NW) cores composed of materials with cubic (In_2O_3,[10,14] Fe_2O_3,[15] and Si[16]) and/or hexagonal (wurtzite ZnO[11−13]) crystal structures. If these NWs or nanorods are initially prearranged in a given pattern, subsequently deposited branches will also be aligned as determined by their orientation relative to the core. For better control of this method of creating aligned NS, one needs to understand the general mechanism of their formation.

In this work, for the first time, we report the formation of highly symmetrical hierarchical ZnO−Ga_2O_3 NS where single-crystal ZnO branches grow not on a core with cubic or hexagonal structure as reported for other branched morphologies but on a low-symmetry monoclinic β-Ga_2O_3 core. ZnO branches grow in six equiangular directions perpendicular to the Ga_2O_3 core, thus yielding the heterostructural morphology of a nanobrush (NB). The branches are arranged regularly and parallel to each other in each row. This regular and symmetrical self-assembly may be used, as shown by our preliminary tests, in the controlled growth of aligned ZnO nanorods with very sharp tips. The main advantages of this method for obtaining aligned ZnO NS are low growth temperature for avoiding thermally induced defects, absence of catalytic impurities, and ZnO nanobranch growth with one end already in contact with an electrically conductive pathway (Ga_2O_3 core). Additionally, we discuss the likely formation mechanism for these NBs.

Experimental Section

Growth of the ZnO−Ga_2O_3 heterostructures was performed in a two-stage process. The first stage involved the growth of Ga_2O_3 NWs by the VLS method[17] on a Si substrate using pure Ga as the source and a 20 nm Au layer as the catalyst in a mixture of Ar and O_2.[19] The second stage involved the growth of ZnO nano arrays on the resultant Ga_2O_3 NWs obtained in the first stage. For this stage, an alumina boat, containing Zn powder and pieces of a silicon substrate with Ga_2O_3 NWs from the first stage, was loaded into a horizontal quartz tube furnace. Zn powder was placed in the hottest zone at the center of the furnace with the Ga_2O_3 NWs in close proximity on the downstream side. The furnace was quickly ramped to 560 °C and held at this temperature under constant Ar flow (1000 mL/min) for 1−2 h and then quickly cooled. To investigate the growth mechanism, second stage experiments were terminated at different time intervals. The resulting

* To whom correspondence should be addressed. E-mail: lena.mazeina@nrl.navy.mil. Phone: 202 404 4520. Fax: 202 764 0546.

10.1021/cg800993b CCC: $40.75
Published on Web 12/22/2008

Report Documentation Page

Form Approved
OMB No. 0704-0188

1. REPORT DATE	2. REPORT TYPE	3. DATES COVERED
NOV 2008		**00-00-2008 to 00-00-2008**

4. TITLE AND SUBTITLE	5a. CONTRACT NUMBER
Controlled Growth of Parallel Oriented ZnO Nanostructural Arrays on Ga2O3 Nanowires	5b. GRANT NUMBER
	5c. PROGRAM ELEMENT NUMBER
6. AUTHOR(S)	5d. PROJECT NUMBER
	5e. TASK NUMBER
	5f. WORK UNIT NUMBER
7. PERFORMING ORGANIZATION NAME(S) AND ADDRESS(ES) **Naval Research Laboratory,Electronics Science and Technology DiVision,4555 Overlook Avenue SW,Washington,DC,20375**	8. PERFORMING ORGANIZATION REPORT NUMBER
9. SPONSORING/MONITORING AGENCY NAME(S) AND ADDRESS(ES)	10. SPONSOR/MONITOR'S ACRONYM(S)
	11. SPONSOR/MONITOR'S REPORT NUMBER(S)

12. DISTRIBUTION/AVAILABILITY STATEMENT
Approved for public release; distribution unlimited

13. SUPPLEMENTARY NOTES

14. ABSTRACT

Novel hierarchical ZnO-Ga2O3 nanostructures were fabricated via a two stage growth process. Nanowires of Ga2O3 were obtained in the first stage by the vapor-liquid-solid mechanism and used as the foundation for growth of self-assembled ordered arrays of ZnO nanostructures during the second stage by the vapor-solid mechanism. The resulting hierarchical nanostructures had a final morphology consisting of nanobrushes (NBs) with Ga2O3 as the core and ZnO as the branches self-assembling symmetrically in six equiangular directions around the core. Characterization of the NBs was performed by scanning and transmission electron microscopies, energy dispersive spectroscopy, and Fourier transform infrared spectroscopy. The mechanism of formation is discussed together with potential applications, among which is the aligned growth of vertically aligned ZnO nanorods that are touted for optoelectronics. Advantages of this alignment method are lower temperature growth, reduced amount of thermally induced defects and absence of catalytic impurities.

15. SUBJECT TERMS

16. SECURITY CLASSIFICATION OF:			17. LIMITATION OF ABSTRACT	18. NUMBER OF PAGES	19a. NAME OF RESPONSIBLE PERSON
a. REPORT	b. ABSTRACT	c. THIS PAGE			
unclassified	**unclassified**	**unclassified**	**Same as Report (SAR)**	**6**	

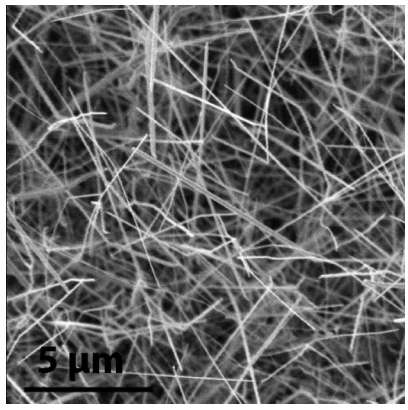

Figure 1. SEM image of Ga_2O_3 nanowires.

samples were analyzed and characterized by Fourier transform infrared spectroscopy (FTIR), scanning electron microscopy (SEM), energy dispersive spectroscopy (EDS) using a LEO SUPRA 55, and transmission electron microscopy (TEM) using a JEOL 2200 also with EDS capabilities.

Results

SEM and TEM analyses showed that the NWs are straight, single crystals largely free of any extended defects (Figure 1), and with diameters of 50−150 nm and lengths of up to hundreds of micrometers. Selected area diffraction (SAD) of numerous NWs confirmed they are monoclinic β-Ga_2O_3 single crystals with $a = 12.23$ Å, $b = 3.04$, $c = 5.80$, $\beta = 103.7°$[18] and elongated along [010] and [100] directions (Figure 2a−d). The number of NWs analyzed by TEM was statistically insufficient to allow the determination of a single preferred growth direction or relative percentages of the two growth directions observed. Larger Ga_2O_3 NWs were elongated along the $[\bar{2}01]$ direction and exhibited surfaces consisting of zigzag (010) and (200) facets (Figure 2g). Zigzag facets were not observed for small NWs but some manner of faceting is expected along the growth axis consisting of planes with low surface energies.[20,21]

The FTIR spectrum (Figure 3) of the ZnO−Ga_2O_3 NBs with short bristles (Figure 4) exhibited bands that matched the known FTIR spectrum of Ga_2O_3: two strong bands at 450 and 670 cm^{-1} (A_u modes), and four weak bands at 517, 613, 720, and 765 cm^{-1} (B_u modes). The positions of these weaker bands, however, are slightly shifted relative to pure Ga_2O_3.[22] Thus, A_u modes of Ga_2O_3, which are polarized to the *b*-axis, a 2-fold axis, dominate the spectrum. B_u modes, which are polarized perpendicular to the *b*-axis, are very weak when compared to the FTIR spectrum of bulk Ga_2O_3 and Ga_2O_3 nanoribbons.[22] In a cylindrical NS, in which the wavelength of the IR light is much greater than the NS diameter, the electric field of the incident IR radiation polarized normal to the cylinder axis is reduced in intensity, inside the NW, by the electrostatic depolarization field.[23] Light polarized parallel to the cylinder axis, on the other hand, is unaffected. On the basis of the above information, we conclude that most of our cylindrically shaped NWs are elongated along the *b*-axis, or [010] direction, in agreement with our TEM observations. Two additional bands at 418 and 578 cm^{-1} (Figure 3) indicate the presence of $ZnGa_2O_4$[24] and will be further addressed later in this paper.

The resulting NS obtained during the second growth stage were brush-like structures exhibiting two morphologies, depending on the duration of the second growth stage. The first morphology type was NBs with short, thick branches ("bristles", Figure 4) and an overall diameter of ∼1 μm. These NBs formed when the second stage lasted for 1−1.5 h. The ZnO bristles grew in parallel arrays perpendicular to the Ga_2O_3 core and exhibited hexagonal ends (Figure 4b) indicating that the bristles grew along the [0001] direction. Initially, these bristles are rather thick (Figure 4c), but they become more elongated and thinner in diameter with continued growth. The overall diameter of the fully formed 6-fold structure increases to 2.5 μm (Figure 4c).

The second morphology type for these NBs has longer branches ("needles", Figure 5) with a tip-to-tip distance of ∼8 μm and was observed when the second growth stage lasted 2 h. These ZnO needles also grow out in six equiangular directions perpendicular to the Ga_2O_3 core as long parallel arrays (Figure 5a,c). The length of these needles are ∼3 μm, and the thicknesses are ∼40−50 nm at the base, 15−17 nm in the middle, and 10−12 nm at the tip (Figure 5b). The length of both types of NBs is determined by the total length of the Ga_2O_3 NW core and reaches several hundreds of micrometers. EDS analysis in the SEM could not detect Ga for either NBs morphology types because of the dense ZnO nanorods arrays surrounding the Ga_2O_3 cores. However, EDS analysis in the TEM confirmed the bristles in the early phases (Figure 6a) and later phases (Figure 7a) of growth are composed purely of Zn and O, whereas the core consisted mostly of Ga and O with typically less than 2 wt % Zn. The ZnO needles, formed during the later phase of growth, showed no variation in the Zn:O ratio along the length of the needle.

TEM verified that both short bristles and long needles grow independently along the [0001] direction (Figures 6b, 7a), a typical growth direction for rod-like ZnO structures.[13] Additionally, SAD analysis along the long axis of the NB showed that each ZnO bristle was oriented with the $[2\bar{1}\bar{1}0]$ direction parallel to the growth direction of the Ga_2O_3 core. High resolution imaging (Figure 7b), where the independently grown ZnO branches have coalesced, show a ∼60° twin boundary. This observation strongly indicates the nucleation and growth of these ZnO nanobranches were near perfectly initiated along equiangular (60°) directions without significant formation of extended defects.

Though FTIR indicated the presence of $ZnGa_2O_4$ in the NBs, TEM analysis could not provide direct confirmation. Neither HRTEM nor SAD of the first stages of growth of NB (Figure 5a,b) could identify lattice fringes or diffraction patterns indicative of the spinel $ZnGa_2O_4$. One reason for the discrepancy is likely that the amount of $ZnGa_2O_4$ present is insufficient to yield a strong signal for either HRTEM or SAD. However, FTIR is a global, averaging approach with higher sensitivity to trace compounds up to 1−2 wt %. Additionally, any $ZnGa_2O_4$ present will likely be confined between the interface of ZnO bristles and the Ga_2O_3 core. The final NB structures are much too thick at the base of the ZnO bristles to conduct HRTEM or even yield SAD spot patterns, even for the Ga_2O_3 core. However, FTIR demonstrates sufficient penetration deep within the NBs to yield signal from the Ga_2O_3 core and likewise from the Ga_2O_3−ZnO interface.

Discussion

On the basis of the combined SEM, TEM, EDS, and FTIR results mentioned above, the following growth mechanism for ZnO−Ga_2O_3 NBs can be proposed. The nucleation of ZnO bristles on the Ga_2O_3 core first occurs either by nucleating directly on the Ga_2O_3 core or through the formation of $ZnGa_2O_4$ (Figures 6a, 8a). It is possible that the metallic Zn reacts with O_2 to form ZnO_x that then reacts with Ga_2O_3 to form a thin layer of $ZnGa_2O_4$ (spinel cubic structure). It is known that

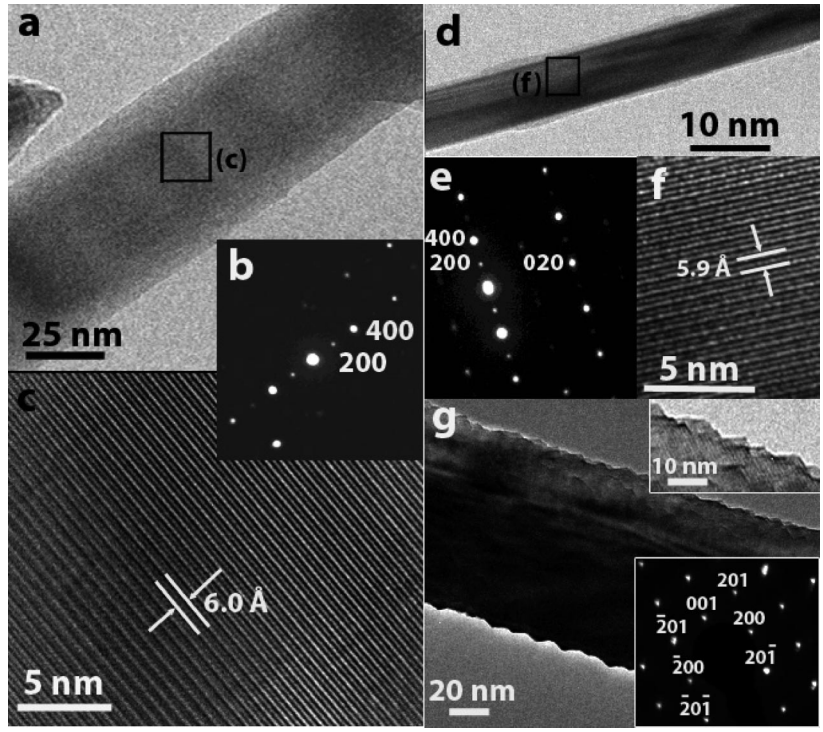

Figure 2. TEM images of Ga_2O_3 NWs with SAD patterns recorded near the [001] zone axis (b,e) and on the [010] zone axis (g, inset). (a) Ga_2O_3 NW and its lattice fringes (c) grown along the [100] direction. (d) Ga_2O_3 NW and its lattice fringes (f) grown along the [010] direction. (g) Ga_2O_3 NW elongated along the [$\bar{2}$01] direction and exhibiting surfaces consisting of zigzag (010) and (200) facets.

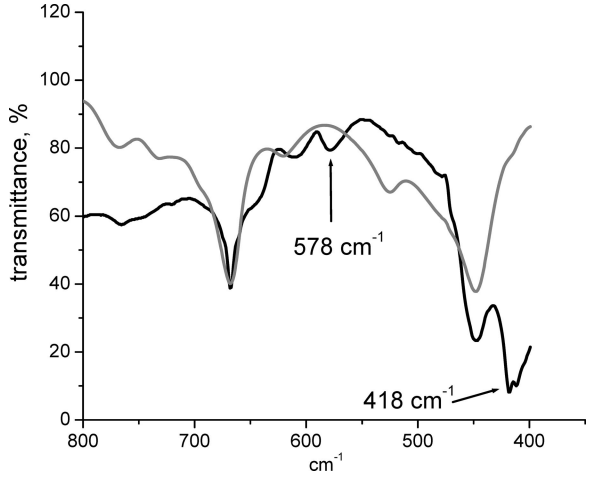

Figure 3. FTIR spectra of pure Ga_2O_3 nanowires (gray) and of ZnO−Ga_2O_3 NBs (black). Bands corresponding to the $ZnGa_2O_4$ are denoted.

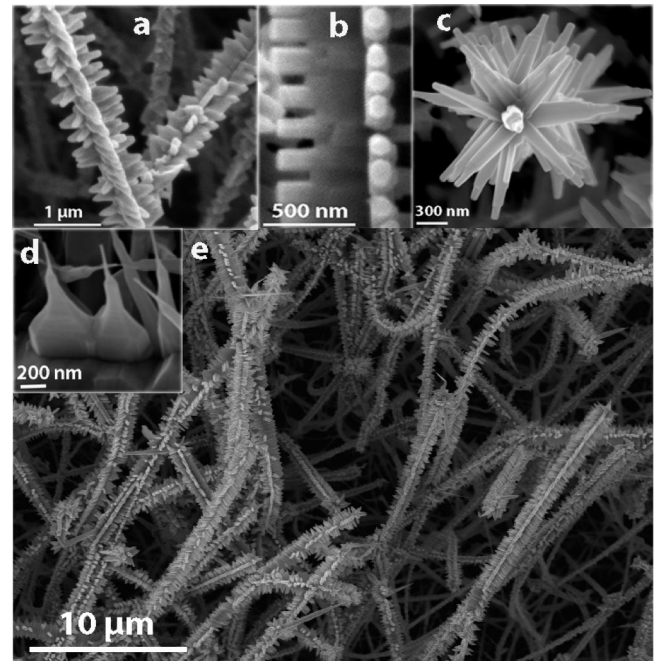

Figure 4. Different stages of growth of Ga_2O_3−ZnO heterostructures: (a) Additional rows of ZnO bristles forming on initially 4-fold NB. (b) First stages of thinning of the bristle with hexagonally shaped ends. (c) Complete 6-fold NB. (d) Intergrown bristle showing elongation and thinning. (e) Low magnification SEM image of the ZnO−Ga_2O_3 NBs to show the abundance.

$ZnGa_2O_4$ forms in the Ga_2O_3−ZnO system even if only a small amount (∼1 at %) of Ga is present in ZnO[25] because $ZnGa_2O_4$ is thermodynamically more stable than a physical mixture of ZnO and Ga_2O_3.[26,27] $ZnGa_2O_4$ is also known to form a solid solution with Ga_2O_3 though with limited solubility[28] which may be responsible for the slight shifts of the weaker Ga_2O_3 bands observed in the FTIR spectrum of these NBs (Figure 3). Additionally, several planes of $ZnGa_2O_4$ and Ga_2O_3 exhibit an epitaxial relationship.[29] It is possible that $ZnGa_2O_4$ nucleates along the Ga_2O_3 NW facets prior to the growth of ZnO bristles serving as a "buffer" layer that accommodates strain between the Ga_2O_3 core and the nucleating ZnO bristles. The $ZnGa_2O_4$ can act as a buffer layer for ZnO growth either by forming a solid solution with ZnO[28,30] or through an epitaxial relationship with ZnO. From a crystallographic standpoint, it can be proposed that the 3-fold symmetry of (111) $ZnGa_2O_4$ would be a good candidate for (0001) ZnO where an approximate lattice mismatch comparing $ZnGa_2O_4$ {20$\bar{2}$} and ZnO {10$\bar{1}$0} is only 5%. Nucleation of ZnO on cubic $ZnGa_2O_4$ rather than directly on

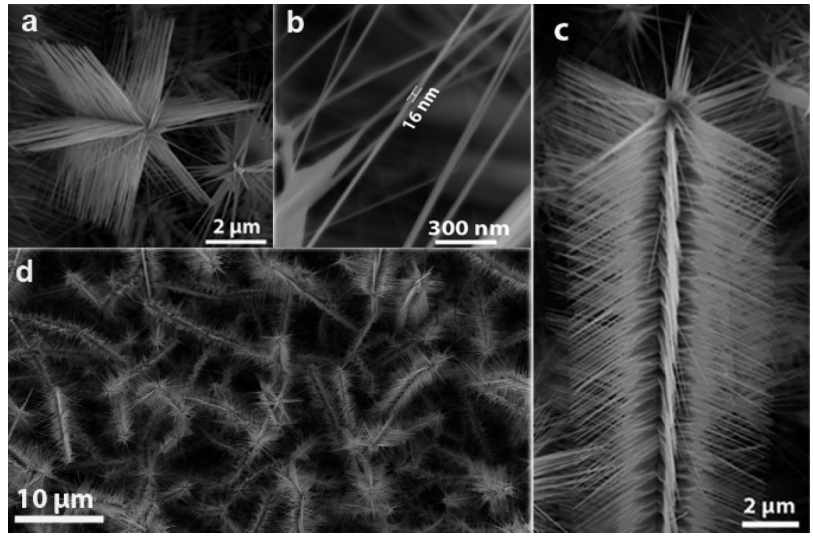

Figure 5. SEM micrograph of NBs with long needles. (a) Six-fold orientation of needles growing in six equiangular directions around the core. (b) High magnification image of needles showing the size in the middle of the needle. (c) Parallel growth of needles along the length of the NB. d) Low magnification SEM image of the ZnO−Ga_2O_3 NBs to show the abundance.

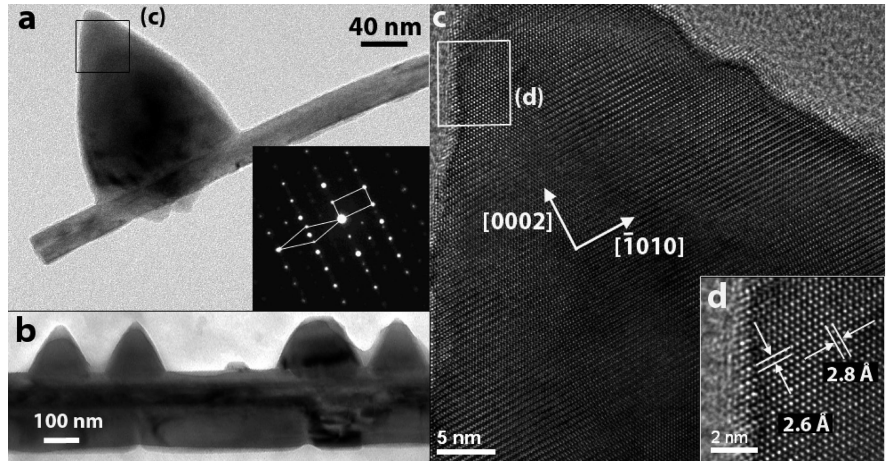

Figure 6. Summary of TEM results for NBs with bristles at the early stages of growth. (a) Single ZnO bristle on the Ga_2O_3 core. Inset shows a diffraction pattern of both the ZnO bristle (rectangle) and the Ga_2O_3 core (diamond) recorded along the [1$\bar{2}$10] ZnO plane axis. (b) Several ZnO bristles growing on a Ga_2O_3 core. (c) Lattice fringes of a ZnO bristle showing that the bristle is a single crystal growing in [0002] direction. (d) Spacing between fringes corresponding to (0002) and (1$\bar{0}$10) planes.

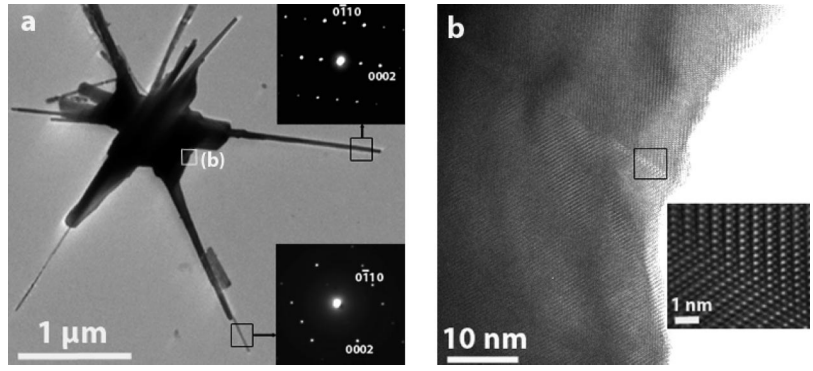

Figure 7. Summary of TEM results for NBs with long bristles (needles). (a) Insets show diffraction patterns of the ZnO needles recorded along the [2$\bar{1}$10] zone axes. (b) Lattice fringes showing intergrowth of ZnO bristles from different rows.

monoclinic Ga_2O_3 might explain the highly symmetric morphology of these NBs since ZnO is known to form similar hierarchical structures on materials with cubic structures.[10−13]

However, it is possible that ZnO nucleates directly on Ga_2O_3, as has been observed elsewhere at lower temepratures.[29] Additionally, {101} and {10$\bar{1}$} Ga_2O_3-surfaces are orthogonal

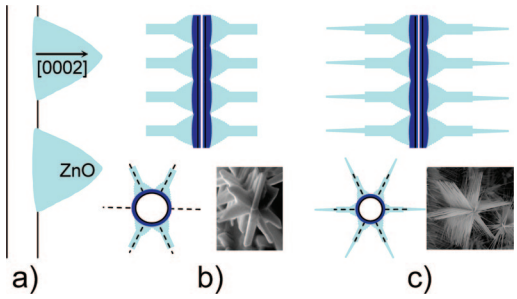

Figure 8. Schematic illustrating the formation of ZnO−Ga_2O_3 NS. (a) ZnO bristles nucleates on Ga_2O_3 core in [0001] direction. (b) Several rows of ZnO bristles form around the core to produce a 4-fold NB with 2-fold symmetry. $ZnGa_2O_4$ (marked as dark blue) and is considered already to be present at this stage. (c) Additional rows of bristles grow in between previously formed four; bristles elongate forming a NB with long needles.

to the [010] growth direction, have nearly 6-fold symmetry, and show lattice mismatch within 6% and 17%, respectively, with (0001) ZnO. Formation of $ZnGa_2O_4$ in this case might happen at later stages of growth by the thermally induced reaction of Ga_2O_3 core and nucleated ZnO bristles (Figure 8b). In either scenario of $ZnGa_2O_4$ formation, the ZnO bristles continue to self-assemble (as shown in Figure 6b) before all the available surface area of the Ga_2O_3 core has been fully either converted to $ZnGa_2O_4$ or covered with ZnO (Figure 8a). After the Ga_2O_3 core is covered completely with short ZnO bristles (Figures 4, 8b), they thin and eventually become needles through a "layer-by-layer" mechanism (Figure 8c).[31] Figure 4d shows that two bristles with needles at the early stages of growth are intergrown suggesting that the elongation process is happening simultaneously with the thickening of the bristles within a single row. Different rows are intergrown as well, indicating the thickening of ZnO bristles is happening in all directions (Figure 7b) creating a thick ZnO shell around the Ga_2O_3 core. Figure 7b demonstrates that every single ZnO bristle along its full length is monocrystalline.

In most heterostructures, we have seen that first a single row of bristles forms at the early stages of growth (Figure 6b). It is possible that the next stage of growth would be a formation of double-sided nanocombs. However, structures with this morphology were not found, probably because they would constitute an intermediate product as would 4-fold NBs analogous to In_2O_3−ZnO NS.[10] Since the formation of the fifth and sixth row of bristles occurs between the previously formed four and yields a highly symmetrical structure, we believe that the 4-fold brushes are not ideally symmetrical and actually have a 2-fold symmetry (Figure 8b). We believe that the 4-fold structures also represent an intermediate product that will eventually convert to a 6-fold symmetry when two additional rows of bristles form between two previously formed rows (Figures 4a, 8b,c). The growth of the fifth and sixth rows of ZnO bristles occurs at the same time as the elongation of the ZnO needles (Figures 4d, 8c). These combined effects produce the observed NBs with long needles. Only 6-fold brushes are found in the second type of growth which is evidence that this type of structure represents the final stage of growth. Even though the layer of Ga_2O_3 nanowires on the substrate is somewhat dense prior to ZnO growth, ZnO appears to successfully diffuse and form bristles on all Ga_2O_3 nanowires. At the same time, even though ZnO NS can be grown directly on the Si substrate with a high yield, we found ZnO branches grew preferentially on the Ga_2O_3. On substrate areas free of Ga_2O_3 little or no ZnO NS growth was observed. This supports the view that ZnO NS growth is energetically more favorable on Ga_2O_3 than on the Si substrate,

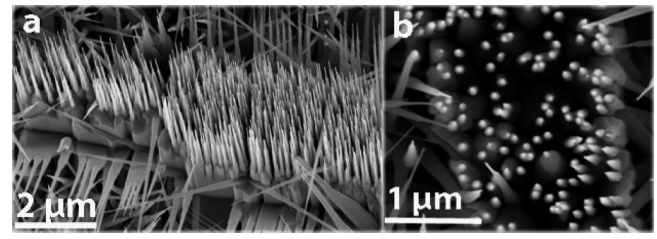

Figure 9. ZnO nanorod arrays grown on β-Ga_2O_3 nanosheet. (a) Side and (b) top views.

possibly enhanced by the energetically more favorable reaction of ZnO with Ga_2O_3 NWs. These observations provide useful insight for obtaining parallel arrays of ZnO nanorods grown on pre-deposited and pre-aligned nanowires or on other NS that can be arranged laterally using recently developed methods.[5,6] Since these branched heterostructures grow symmetrically around the core, different alignments of ZnO needles are possible, for example, simultaneously parallel and perpendicular to the surface. This organized morphology could be useful in applications such as surface enhanced Raman spectroscopy (SERS), where it has been shown that the Raman signal can be significantly enhanced in the case of crossed and closely spaced parallel dielectric wire/Ag composites.[32,33]

Depending on the desired length and thickness, the growth of ZnO bristles or needles may be controlled by the density of the pre-deposited Ga_2O_3 NWs and by the initial amount of Zn powder (controlling the total Zn vapor concentration). To avoid or minimize lateral branching of ZnO needles, one can grow ZnO on structures with well-defined surfaces such as nanobelts, nanoribbons, nanosheets,[34] or even single crystal Ga_2O_3 thin films.[35] Our preliminary tests on Ga_2O_3 nanosheets showed that ZnO arrays grow vertically and arrayed parallel to each other (Figure 9).

For this 2-stage method of aligning ZnO nanorods, a significant advantage is the low growth temperature. Many methods for obtaining vertically aligned and ordered patterns of ZnO nanorods require temperatures above 800 °C.[2] Our two-stage method requires a lower temperature (560 °C) and enhances the potential for application of these structures in nanoscale electronic devices by permitting growth without the accompanying formation of thermally induced extended defects. Another important factor is that the resulting ZnO arrays are automatically in contact with a conductive pathway (Ga_2O_3 core). Also, this method of aligned growth eliminates impurities from a catalyst since the growth occurs by a self-assembly VS mechanism. Additionally, a Ga_2O_3 nano core with ZnO rods extending from the surface can exhibit even higher conductivity than that of pure Ga_2O_3 as has been observed for other heterostructures.[36] Further investigations of ZnO−Ga_2O_3 NS applications are underway, and a discussion of their gas sensing properties will be reported in a future work. Since there is no evidence that $ZnGa_2O_4$ is present at the outer surfaces of the NBs (both the bristles and the outer shell of the NB core are purely ZnO), we expect little influence from any trace amounts of $ZnGa_2O_4$ on the surface-dominated gas sensing properties of these NBs.

Conclusions

Novel ZnO−Ga_2O_3 hierarchical heterostructures are reported for the first time, where ZnO branches are symmetrically oriented in parallel arrays around a monoclinic Ga_2O_3 core. They were synthesized by a two stage process: Ga_2O_3 nanowires were

grown first by the VLS process, and then ZnO branches were grown on the Ga_2O_3 NWs by the VS process, resulting in structures having the morphology of nanobrushes (NBs). Evidence of $ZnGa_2O_4$ by FTIR analysis indicates nucleation of $ZnGa_2O_4$ on the Ga_2O_3 core that acts as a transition phase to the eventual growth of ZnO branches. Individual ZnO bristles grow independently along the [0001] direction with the $[2\bar{1}\bar{1}0]$ direction consistently parallel to the Ga_2O_3 core growth direction. Since the ZnO branches grow perpendicular to the core in equiangular directions, the resulting NBs morphology exhibits highly symmetrical morphologies. The length of the ZnO branches and the symmetry of the NB depend on the growth duration and initial density of Ga_2O_3 nanowires. ZnO branches grow perpendicular to the core in equiangular directions and parallel to each other along the core. This self-assembly process can be used for creating arrays of ZnO on Ga_2O_3 surfaces. Compared to conventional techniques, the advantages of the two-stage growth method in this study are that the ZnO nanobranches grow with one end already in contact with a conductive pathway (Ga_2O_3 core) and that no catalyst is needed, thus eliminating a potential source of contamination. Additionally, this method produces ZnO nanorods with extremely sharp tips which is important for field emission devices. Another very important advantage is the relatively low temperature (560 °C) at which the vertically aligned ZnO rods grow, enhancing the possibility for fabricating ZnO-based nanoelectronic devices by allowing growth without the accompanying formation of thermally induced defects.

Acknowledgment. Victor Bermudez and Keith Perkins are thanked for useful discussions. This work was supported by the Office of Naval Research. L.M. and Y.N.P. thank the National Research Council for financial support through the Research Associateship Program.

References

(1) Chang, K.-W.; Wu, J.-J. *J. Phys. Chem. B* **2004**, *108*, 1838–1843.
(2) Fan, H. J.; Fleischer, F.; Lee, W.; Nielsch, K.; Scholz, R.; Zacharias, M.; Goesele, U.; Dadgar, A.; Krost, A. *Superlattices Microstruct.* **2004**, *36*, 95–105.
(3) Yi, G.-C.; Wang, C.; Park, W. *Semicond. Sci. Technol.* **2005**, *20*, S22–S34.
(4) Park, W. I.; Yi, G.-C.; Kim, J.-W.; Park, S.-M. *Appl. Phys. Lett.* **2003**, *82*, 4358–4360.
(5) Moore, D.; Morber, J. R.; Snyder, R. L.; Wang, Z. L. *J. Phys. Chem.* **2008**, *112*, 2895–2903.
(6) Whang, D.; Jin, S.; Lieber, C. M. *Nano Lett.* **2003**, *3*, 951–954.
(7) Hangarter, C. M.; Rheem, Y.; Yoo, B.; Yang, E.-H.; Myung, N. V. *Nanotechnology* **2007**, *18*, 205305/1–205305/7.
(8) Schmidt-Mende, L.; MacManus-Driscoll, J. L. *Mater. Today* **2007**, *5*, 40–48.
(9) Goepel, W. *Ber. Bunsen-Ges.* **1978**, *82*, 744–756.
(10) Lao, J. Y.; Wen, J. G.; Ren, Z. F. *Nano Lett.* **2002**, *2*, 1287–1291.
(11) Gao, P.; Wang, Z. L. *J. Phys. Chem. B* **2002**, *106*, 12653–12658.
(12) Kuan, C. Y.; Chou, J. M.; Leu, I. C.; Hon, M. H. *J. Solid State Chem.* **2008**, *181*, 673–678.
(13) Zhong, L. W. *Mater. Today* **2004**, *6*, 26–33.
(14) Xu, L.; Su, Y.; Li, S.; Chen, Y.; Zhou, Q.; Yin, S.; Yi, F. *J. Phys. Chem. B* **2007**, *111*, 760–767.
(15) Zhang, D.-F.; Sun, L.-D.; Jia, C.-J.; Yan, Z.-G.; You, L.-P.; Yan, C.-H. *J. Am. Chem. Soc.* **2005**, *127*, 13492–13493.
(16) Lugstein, A.; Andrews, A. M.; Steinmair, M.; Hyun, Y.-J.; Bertagnolli, E.; Weil, M.; Pongratz, P.; Schramboeck, M.; Roch, T.; Strasser, G. *Nanotechnology* **2007**, *18*, 355306/1–355306/5.
(17) Wagner, R. S.; Ellis, W. C. *Appl. Phys. Lett.* **1964**, *4*, 89–90.
(18) Geller, S. *J. Chem. Phys.* **1960**, *33*, 676–684.
(19) Prokes, S. M.; Carlos, W. E.; Glembocki, O. J. *Proc. SPIE Int. Soc. Opt. Eng.* **2005**, *6008*, 60080C/1–60080C/10.
(20) Justo, J. F.; Menezes, R. D.; Assali, L. V. C. *Phys. Rev. B* **2007**, *75*, 045303/1–045303/5.
(21) Menezes, R. D.; Justo, J. F.; Assali, L. C. V. *Phys. Status Solidi* **2007**, *204*, 951–955.
(22) Bermudez, V. M.; Prokes, S. M. *Langmuir* **2007**, *23*, 12566–12576.
(23) Kittel, C. *Introduction to Solid State Physics*; Wiley Publishers: New York, 1967.
(24) Van Gorkom, G. G. P.; Haanstra, J. H.; Van den Boom, H. *J. Raman Spectrosc.* **1973**, *1*, 513–519.
(25) Goncalves, A.; Marques de Lima, S. A.; Davolos, M. R.; Antonio, S. G.; Paiva-Santos, C. *J. Solid State Chem.* **2006**, *179*, 1330–1334.
(26) Katayama, I.; Iseda, A.; Kemori, N.; Kozuka, Z. *Trans. Jpn. Inst. Met.* **1982**, *23*, 556–562.
(27) Navrotsky, A.; Kleppa, O. J. *J. Inorg. Nucl. Chem.* **1968**, *30*, 479–498.
(28) Li, C.; Zhang, X.; Wu, G.; Guan, D. *Faguang Xuebao* **2006**, *27*, 963–966.
(29) Chang, K.-W.; Wu, J.-J. *J. Phys. Chem. B* **2005**, *109*, 13572–13577.
(30) Moon, J.-W.; Moon, H.-S.; Oh, E. S.; Kang, H. I.; Kim, J. S.; Park, H. L.; Kim, T. W. *Int. J. Inorg. Mater.* **2001**, *3*, 575–578.
(31) Yang, Y. H.; Wang, B.; Yang, G. W. *Nanotechnology* **2006**, *17*, 5556–5560.
(32) Prokes, S. M.; Glembocki, O. J.; Rendell, R. W.; Ancona, M. G. *Appl. Phys. Lett.* **2007**, *90*, 093105/1−093105/3.
(33) Prokes, S. M.; Park, H. D.; Glembocki, O. J.; Alexson, D.; Redell, R. W. *Proc. SPIE* **2007**, *6768*, 67680E1–67680E13.
(34) Wang, G.; Park, J.; Kong, X.; Wilson, P. R.; Chen, Z.; Ahn, J. *Cryst. Growth Des.* **2008**, *8*, 1940–1944.
(35) Oshima, T.; Arai, N.; Suzuki, N.; Ohira, S.; Fujita, S. *Thin Solid Films* **2008**, *516*, 5768–5771.
(36) Wang, J. X.; Sun, X. W.; Xie, S. S.; Yang, Y.; Chen, H. Y.; Lo, G. Q.; Kwong, D. L. *J. Phys. Chem. C* **2007**, *111*, 7671–7675.

CG800993B